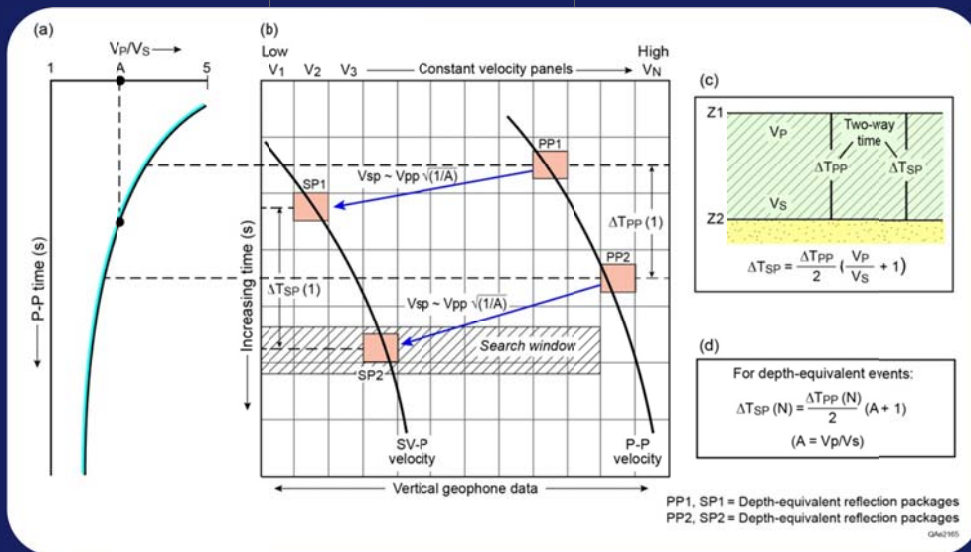


A report to the sponsors of the  
Exploration Geophysics Laboratory

# Guidelines for Selecting Legacy P-Wave Data for SV-P Data Processing

Bob Hardage, Michael DeAngelo,  
and Donald Wagner



March 2015



BUREAU OF  
ECONOMIC  
GEOLOGY

# **Guidelines for Selecting Legacy P-Wave Data for SV-P Data Processing**

**Bob Hardage, Michael DeAngelo, and Donald Wagner**

**March 2015**

## **Abstract**

There are several criteria that need to be satisfied and several investigations that need to be done to determine if legacy P-P data at a site of interest are appropriate for SV-P data processing. This report summarizes procedures that are currently practiced by the Exploration Geophysics Laboratory (EGL) to determine if SV-P data processing should, or should not, be initiated for a particular P-P seismic survey. These procedures are applied to a 3D seismic survey acquired in Scott County, Kansas, to illustrate our data-evaluation process in action. The failure of these particular Scott County legacy data to satisfy some key criteria required for SV-P data processing led to a decision to not initiate SV-P processing of the legacy P-P data available at this site.

## **Introduction**

A 22-mi<sup>2</sup> 3D P-P survey located in Scott County, Kansas, was offered to EGL as a candidate survey for SV-P data processing of vertical-geophone data. These legacy P-P data provided an opportunity for the Exploration Geophysics Laboratory (EGL) to apply data-qualification procedures to determine if it was prudent to initiate an SV-P data-processing effort with these particular P-P data. This report illustrates the procedures that were applied to evaluate these legacy data and the results that led to a decision to not initiate SV-P data processing.

The decision criteria that were applied to these legacy P-P data are discussed in the following report sections and are numbered for ease of reference. This numbering scheme does not imply any order of priority for the data-qualification requirements. The criteria that guide EGL's logic in deciding if a particular legacy P-P seismic survey should be subjected to SV-P data processing are then assembled into a single-page format in Table 1 at the end of the report. This concise spreadsheet should be a convenient document for others to refer to as they consider the advisability of initiating SV-P processing of other legacy P-P data.

## Decision Criteria

### Criterion 1 - Trace Length

When evaluating legacy P-P data for SV-P data processing, it is essential to determine if the length of the recorded P-P data traces is sufficient to include SV-P reflections from the deepest target of interest. If the P-P reflection from the deepest imaging objective appears at an image time of  $T_{PP}$  milliseconds, then the SV-P reflection from that same interface should appear at an image time  $T_{SP}$ , where

$$(1) \quad T_{SP} = 0.5(1 + V_P/V_S)T_{PP}.$$

In this equation,  $V_P$  is the average P-wave velocity to the deepest target, and  $V_S$  is the average S-wave velocity to that same depth. If there are no real data (either dipole sonic logs or VSP data) to quantify  $V_P$  and  $V_S$  velocities, then a person simply has to guess what the  $V_P/V_S$  velocity ratio should be at the prospect of interest. When forced to assume a value of  $V_P/V_S$  without the guidance of real data, it is prudent for purposes of trace-length qualification of the data to estimate a  $V_P/V_S$  value that is slightly higher than what  $V_P/V_S$  normal behavior is expected to be.

The times  $T_{PP}$  and  $T_{SP}$  used in Equation 1 are 2-way vertical travel times. The length of candidate P-P data traces should exceed this  $T_{SP}$  vertical image time by a factor of  $1/[\cos(45^\circ)]$  to ensure that reflections that follow slant paths between source and receiver stations separated a distance equal to twice the depth of the deepest target of interest can be utilized. Raypaths involving source and receiver stations at these maximum offsets would have incident angles of  $45^\circ$  at the deepest interface. Thus, the length of recorded P-P data traces ( $T_{LENGTH}$ ) should be at least a factor of 1.4 greater than the  $T_{SP}$  value shown in Equation 1, meaning

$$(2) \quad T_{LENGTH} = 0.7(1 + V_P/V_S)T_{PP},$$

P-P trace lengths greater than  $T_{LENGTH}$  would be even more desirable, particularly when structural dip is involved.

### Application of Criterion 1 to Scott County Data

The trace length for the Scott County P-P data was 2 sec, and the deepest P-P reflection of interest occurred at a P-P vertical travel time  $T_{PP} = 0.95$  sec. Local dipole sonic log data indicated the average value of the  $V_P/V_S$  velocity ratio at this legacy-data site was approximately 2. Thus applying the equation  $T_{SP} = 0.5(1 + V_P/V_S)T_{PP}$  leads to the conclusion that this same deep target would occur at approximately a SV-P vertical travel time of  $T_{SP} = 1.42$  sec in SV-P image space. The time coordinates of reflections from this deep target at far offsets (offsets associated with take-off angles that are  $45^\circ$  from vertical) would be  $T_{SP}/\cos(45^\circ) = 2$  sec. An alternate calculation is  $0.7(1 + V_P/V_S)T_{PP} = 2$  sec. Thus the trace length of the Scott County P-P data (2 sec) is barely acceptable for SV-P processing. A trace length greater than 2 sec would be preferred.

## **Criterion 2 – SV-P Data Acquisition Footprint**

The source-receiver geometry used to record P-P data being considered for SV-P data processing should be analyzed to determine if that acquisition geometry imposes undesired data-acquisition footprint effects in SV-P data. An **acquisition footprint** can be defined as *an anomalous behavior of a seismic attribute that appears as a geometrical pattern across seismic image space that matches the geometrical pattern of the source and receiver lines that acquired the data*. Some geological features may align with short segments of a few source and/or receiver lines, but seismic attribute trends that exactly match the geometrical patterns of source and receiver lines across an extensive area cannot be portraying realistic geology. Such data artifacts are created by the data-acquisition geometry rather than by geological conditions. In analyzing effects introduced into SV-P data by source-receiver geometry, the common definition of **acquisition footprint** given above can be expanded to include *any erratic behavior of SV-P stacking fold that occurs in an acquisition geometry when that same acquisition geometry produces a P-P stacking fold that is smooth and regular*.

It is common for some source and receiver line geometries to not produce an acquisition footprint in common-midpoint (CMP) data P-P data, and yet generate an obvious acquisition footprint in converted-mode (CCP) data. This situation is encountered more frequently in older vintage 3D seismic programs that were acquired before serious thought was given to implementing source and receiver geometries that were more accommodating for both CMP and converted-mode data. Although the possibility of unwanted acquisition footprint effects in SV-P data needs to be investigated when evaluating any legacy 3D P-P data for SV-P data processing, it is particularly important to do so for older data.

Usually the best way to recognize that an acquisition footprint effect is embedded in recorded data is to calculate map views of stacking fold patterns across seismic image space. An analysis of SV-P stacking-fold for a given source-receiver geometry utilizes the same seismic-design software that is used to quantify P-P and P-SV stacking folds. The only change required in applying this survey-design software to an analysis of SV-P data is that the  $V_p/V_s$  velocity ratio used to examine P-SV imaging conditions has to be inverted to  $V_s/V_p$  to analyze SV-P acquisition footprints. In other words, if a  $V_p/V_s$  value of 2 is used to create map views of P-SV stacking fold, then the same survey-design software will create map views of SV-P stacking fold if the velocity ratio is changed to 0.5.

Frequently a survey-design analysis will show that both P-SV and SV-P data have a stronger acquisition footprint than do their companion P-P data. This outcome does not necessarily mean SV-P data processing should not be attempted. Rather it indicates the size of the superbin that should be used to create SV-P stacked data so that SV-P stacking fold and offset parameters become reasonably smooth across SV-P image space. If SV-P superbin processing has to be implemented, we often see no problem in interpolating SV-P data constructed with modest-size superbins to create SV-P data with normal-size bins. The decisions whether to do such interpolation and how to do that interpolation will vary from seismic survey to seismic survey and from data processor to data processor.

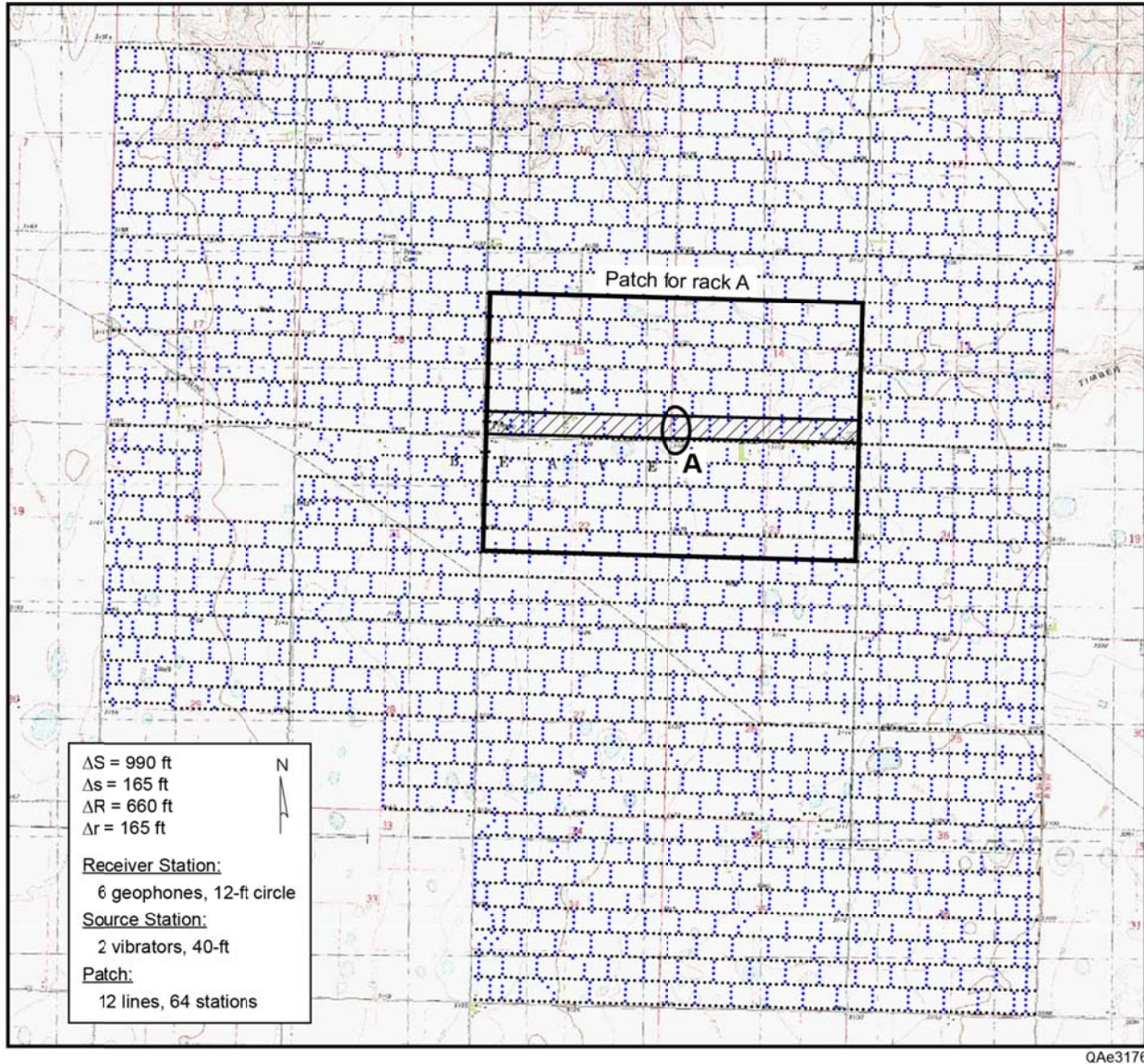


Figure 1. Source-receiver geometry used to acquire the Scott County P-P data.  $\Delta R$  = receiver line interval,  $\Delta r$  = receiver station interval,  $\Delta S$  = source line interval, and  $\Delta s$  = source station interval.

### **Application of Criterion 2 to Scott County Data**

The orthogonal-brick source-receiver geometry used to record the Scott County P-P data is illustrated in Figure 1. Receiver lines were oriented east-west and were separated by intervals of 660 ft in the north-south direction. Source lines were oriented north-south to form an orthogonal brick pattern, and adjacent source-line segments were separated 990 ft in the east-west direction. Source stations and receiver stations were positioned at intervals of 165 ft along these orthogonal source/receiver lines. The recording patch spanned 12 receiver lines (north-south) and extended across 64 receiver stations on each of these 12 lines (east-west). An

example recording patch is shown in Figure 1 centered on source rack **A** near the center of the survey area.

Stacking fold behavior will be used in this report to judge the severity of acquisition footprints in the Scott County data acquired with this source-receiver geometry. Azimuth distributions and offset distributions should also be calculated in rigorous analyses of source-receiver acquisition geometries, but these additional data-acquisition attributes will not be included in this analysis. P-P, P-SV, and SV-P stacking folds associated with the Scott County acquisition geometry are displayed in Figure 2. Note a different color bar is used for the P-P data (Figure 2a) than for the converted-mode data (Figures 2b and 2c). The stacking folds for all three modes are approximately the same, but their fold equivalences can be missed if their respective color bar scales are not considered. Note in the large-scale views in Figure 2, that areas of low SV-P fold (Figure 2c) correspond to the same areas where P-P fold is low (Figure 2a). P-SV fold (Figure 2b) does not mimic P-P fold in the way that SV-P fold does.

No attributes related to P-SV data will be shown in the remainder of this report because horizontal geophones must be deployed to acquire P-SV data, and only vertical geophones were used to record the Scott County data. Although the “big picture” views in Figure 2 may imply to some that P-P and SV-P stacking folds have approximately equivalent smoothness, detailed zoom views of these fold maps tell a different story.

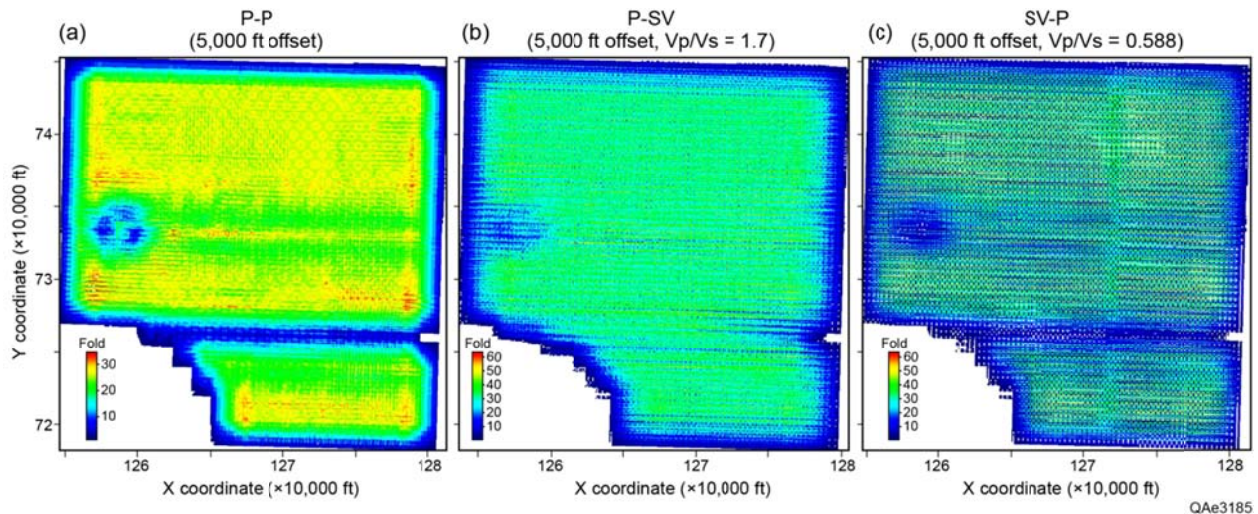


Figure 2. (a) P-P, (b) P-SV, and (c) SV-P stacking folds produced by the acquisition geometry defined in Figure 1. Note the difference in the scales used for the color bars. The converted-mode color bars differ from the P-P color because small areas across each converted-mode image space have folds greater than 50.

An example zoom view of the central area of the fold maps is displayed as Figure 3. These detailed views show that the magnitude of SV-P fold varies erratically from bin to bin compared to the relatively smooth behavior of P-P fold. These irregularities in SV-P stacking fold are an example of a data-acquisition footprint effect that can affect SV-P data processing. In this

instance, the implication is that although P-P data can be processed as 1 X 1 normal bins (82.5 ft X 82.5 ft) and still maintain a smooth stacking fold, SV-P data should be processed as 2 X 2 superbins (165 ft X 165 ft) as a minimum to produce a reasonably smooth stacking fold (and maybe even as larger-size bins). These large-bin data can then be interpolated to normal-bin SV-P data (82.5 ft X 82.5 ft). Some data processors may decide to increase SV-P bin size to a 4 X 4 superbin (330 ft X 330 ft) or even to a 5 X 5 (412.5 ft) X (412.5 ft) superbin. However, the SV-P fold distribution in Figure 3b implies that bins of 165 ft X 165 ft should produce reasonably uniform SV-P fold. No serious penalty should be incurred by processing the Scott County SV-P data as 2 X 2 (or larger) superbin data and then interpolating to normal-size bins.

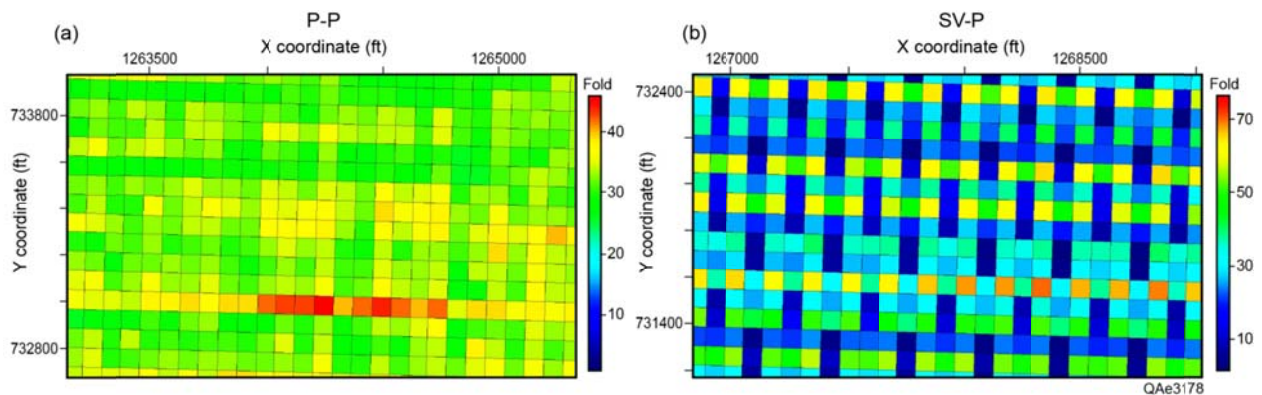


Figure 3. Zoom views of (a) P-P and (b) SV-P stacking fold. Each stacking bin has dimensions of 82.5 ft X 82.5 ft. These data windows are located in the central part of the image space. Each Y axis spans a distance slightly less than two receiver-line intervals, and each X-axis spans a distance slightly greater than two source-line intervals (Figure 1).

The stacking fold maps in Figure 3 show stacking folds for the deepest imaging depths. The severity of an acquisition footprint increases as stacking fold is examined at shallower depths. Thus calculations of SV-P stacking fold should be done at a shallow depth and at a mid-range depth in addition to the deepest depth. If a drilling target is limited to only one formation, then it is probably sufficient to limit a footprint analysis to only that one target depth. Because only one drilling target was of interest at this Scott County site, and that target was at a deep image depth, the analyses presented in Figures 2 and 3 are sufficient to conclude that the SV-P acquisition footprint for the Scott County data is not ideal, but it should be acceptable. This SV-P data-acquisition footprint behavior should not by itself dictate that SV-P data processing should not be attempted.

It is a judgment call as to what magnitude of acquisition-footprint effect is acceptable and what magnitude requires a “do not initiate SV-P processing” conclusion. The decision as to whether to go forward or to abandon an SV-P data processing effort should involve input from one or more competent seismic data processors. For example, some data processors may advise that SV-P processing of the Scott County P-P data should not be initiated given the degree of acquisition footprint that will be involved in the data processing. We at EGL would proceed with SV-P data processing using appropriate size super bins.

### **Criterion 3 - Low-Frequency Energy in the Illuminating Wavefield**

EGL has found that if there is not a rich amount of low-frequency energy in an illuminating wavefield produced by a P-wave source, there is a reduced probability that there will be robust SV-P reflections in vertical-geophone data. If the P source is a shot-hole explosive or a vertical impact, there is usually an attractive amount of low-frequency energy in shot gathers. The likelihood that weak energy levels exist in the lower frequency range of seismic field data increases when the source is a vertical vibrator because lower frequencies can then be deliberately excluded from illuminating wavefields. The likelihood that vibrator data will be deliberately designed to exclude low frequencies is high if data-acquisition decisions do not consider: (1) a direct-S mode will be produced by vertical vibrators, and (2) SV-P data may need to be utilized in addition to P-P data. Thus the comments here focus only on vibrator-source P-wave data because vibrators were used to create the Scott County data.

Two vibrator-sweep parameters are of particular interest when deciding if vibrator-source data are candidates for extracting SV-P reflections. Parameter 1 is the frequency assigned as the low-frequency end of the vibrator sweep. For generating SV-P data, the optimal choice for the low-end of a vibrator sweep is a frequency that starts at 6-Hz or lower (a 4-Hz low-end is ideal). If a vibrator sweep starts at 10-Hz or higher, there can be a serious reduction in the low-frequency components needed to produce good-quality SV-P reflections. Much legacy P-P data have been acquired using vibrator sweeps that start at 10 Hz.

Parameter 2 is the sweep rate. Non-linear vibrator sweeps are not good for generating optimal-quality SV-P reflections because the sweep traverses lower frequencies rapidly and dwells longer at higher frequencies. Given a choice of P-P data acquired with a linear sweep rate or P-P data acquired with a non-linear sweep rate, EGL will opt for the linear-rate data every time. Non-linear sweeps rush through the low-frequency portion of the signal spectrum so fast that robust low-frequency data often do not exist in the illuminating wavefield.

### **Application of Criterion 3 to the Scott County Data**

For the Scott County data, the vibrator sweep range was 12 to 128 Hz, and the sweep was nonlinear at a 3dB per octave rate. Both of these sweep parameters are undesirable for generating robust SV-P data. One could decide at this point that it would be a mistake to attempt to extract SV-P reflections from the Scott County data. However, it is prudent to do a modest amount of data analysis to confirm if this concern is justified. One obvious data procedure would be to compute frequency spectra for several sets of trace gathers. A calculation of the frequency content of the Scott County P-P data is illustrated in Figure 4. This frequency spectrum confirms that important low-frequency components are not embedded in the vertical-geophone data.

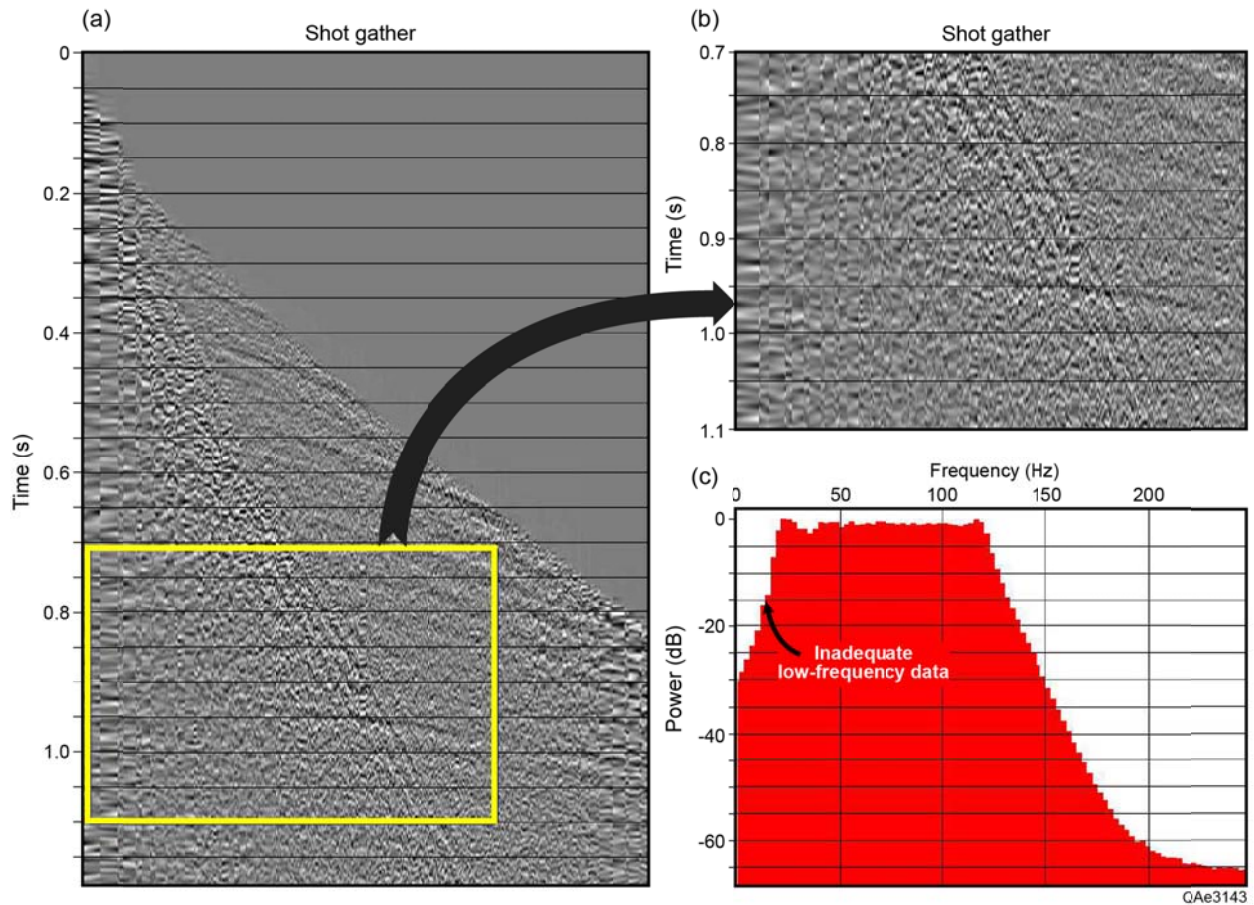


Figure 4. (a) Trace gather of vertical-geophone data acquired at the Scott County study site. The outlined data window spans bold reflections associated with the reservoir target. (b) Zoom view of target-reflection window. (c) Frequency spectrum calculated for the data inside the analysis window. Critical low-frequency components needed for robust SV-P reflections are absent.

Even if a frequency spectrum calculation indicates SV-P reflections will not be robust, as Figure 4c indicates will be the case at the Scott County site, it is still important to inspect constant-velocity stacks of vertical-geophone data if at all possible. In our investigation, we requested CMP stacking velocity panels from the company that processed the Scott County data. These constant-velocity panels allowed us to confirm our concerns that the vibrator sweep parameters used for the Scott County data resulted in poor-quality SV-P reflections.

Examples of vertical geophone stacking-velocity panels of the Scott County data are exhibited as Figure 5. These data show a bold P-P reflection ( $A_{PP}$ ) for the deepest target of interest. Using local dipole sonic log information that identifies the average  $V_p/V_s$  value as 2, the position of the corresponding SV-P reflection ( $A_{SP}$ ) can be calculated. The time-conversion equation relating  $A_{PP}$  and  $A_{SP}$  is shown as the bottom line in the label block in each velocity panel. Visual inspection of the velocity panels shows that there is at best only a faint hint of a reflection event inside the calculated search window (window  $A_{SP}$ ) even though the  $A_{SP}$  window in Figure 5b is moved slightly toward higher velocities to enclose possible reflection energy. The

poor signal-to-noise quality of the data inside each SV-P reflection search window confirmed our suspicion that the weak amount of low-frequency energy in the Scott County data would not allow a successful SV-P data-processing effort. The calculation procedure that identifies SV-P reflection search windows in CMP constant-velocity panel of vertical-geophone data will be discussed later when Criterion 7 (Signal-to-Noise Character of SV-P Reflections) is considered.

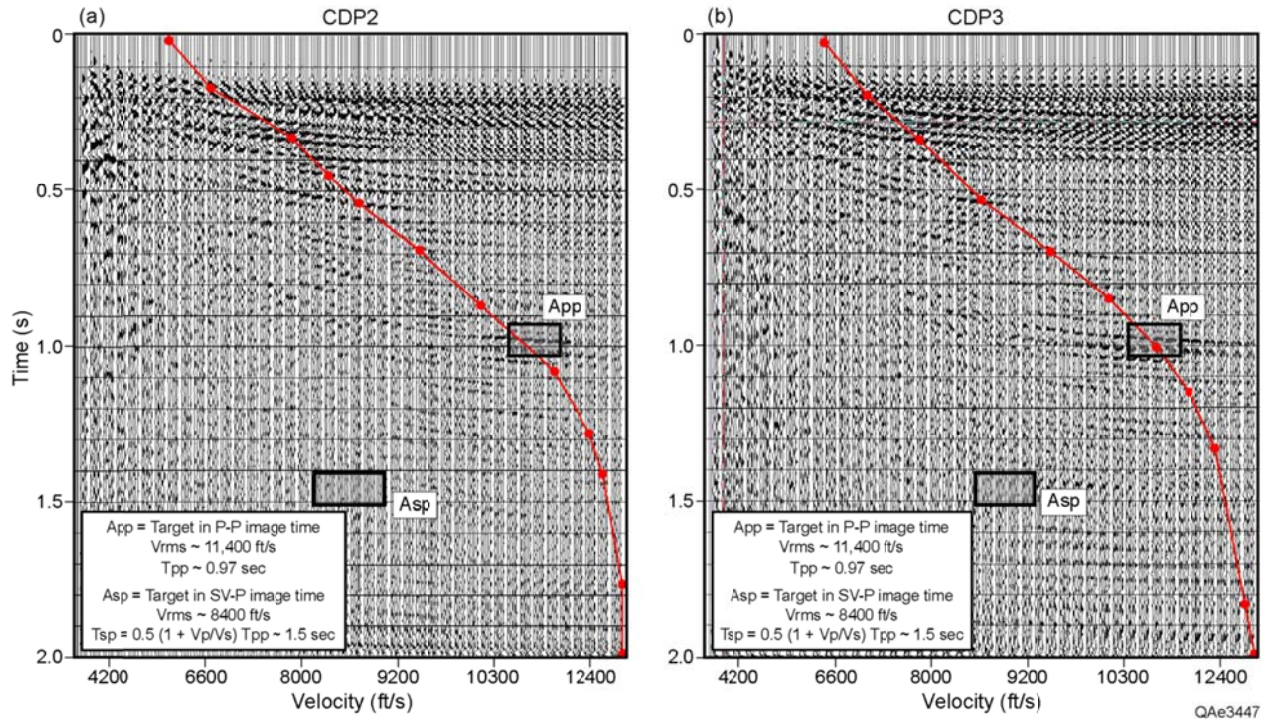


Figure 5. (a) CMP-based constant-velocity panel generated at CDP 2 for the Scott County survey. Event  $A_{pp}$  is the P-P reflection from the deepest target of interest. Based on well log information that  $V_p/V_s = 2$ , the SV-P reflection from this same interface should be located at position  $A_{sp}$ . The absence of reflections inside the  $A_{sp}$  search window confirms that the vibrator sweep parameters used for the Scott County data acquisition did not produce sufficient low-frequency energy. (b) Repeat constant-velocity panels calculated at CDP 3 with the  $A_{sp}$  window moved slightly to the right. Result is the same – only weak evidence of SV-P reflections exists.

#### **Criterion 4 - Estimating S-Wave Statics at Source Stations**

For some legacy P-P data, the most challenging step of extracting SV-P reflections is estimating S-wave statics from vertical-geophone data. S statics are needed to set a common datum for the downgoing illuminating SV wavefield at all source stations across a legacy survey area. If P-P data being considered for SV-P data processing are known to have challenging P-wave static issues, those P-P data are poor candidates for SV-P imaging. If the estimation of P-wave statics is difficult for a particular data set, then determining S-wave statics from the same vertical-geophone data will be even more difficult. If P-wave data from two locations are being considered for SV-P data processing, EGL will always choose the site that has the fewer static-estimation issues.

### **Application of Criterion 4 to Scott County Data**

P-wave static estimation was stated to not be a serious data-processing challenge for the Scott County data. However, we could not determine if S-wave static estimation would also be simple. Because we demonstrated that SV-P reflections would have poor signal-to-noise character because of the weak low-frequency energy in the illuminating SV-P wavefield (Figures 4 and 5), no effort was expended to investigate S-wave static issues at this Scott County site. It would be impossible to investigate S-wave static issues with such poor quality data. S-wave static estimation using vertical-geophone data will thus have to be a subject of a later EGL report.

### **Criterion 5 - Construction of Synthetic Shot Gathers**

If detailed  $V_p$  and  $V_s$  velocity information is available at a prospect where SV-P processing of P-P data is desired, it is important to use this velocity information to do full-elastic modeling of the wave modes that should exist in the data. EGL uses  $V_p$  and  $V_s$  dipole-sonic-log information from local calibration wells to construct both 1D synthetic seismograms and 2D synthetic shot records that illustrate if, and how, P-P and SV-P reflections interfere with each other in vertical-geophone data. The optimal information needed for this modeling is provided by a dipole sonic log, but detailed interval velocities can also be provided by VSP data. 2D synthetic shot gathers are particularly important to data processors because the data allow processors to test strategies for separating SV-P and P-P wavefields.

Significant computational resources are required to do 2D full-elastic modeling, and such resources may not be available to some explorationists. Good-quality, full-elastic modeling codes exist in several seismic data-processing shops, research organizations, and oil/gas companies. Any of these modeling options can be used. EGL can also perform a reasonable amount of 2D modeling analysis for companies that need assistance in evaluating legacy P-P data for SV-P data processing. Simple, low-cost, 1D P-P and SV-P synthetic seismograms can also be helpful for identifying interferences between SV-P reflections from shallow interfaces and P-P reflections from deeper interfaces, and may in some cases be sufficient to identify interference between P-P and SV-P reflection events. The shortcoming of 1D modeling is that the data do not show how P-P and SV-P reflections interfere over the full offset range of seismic data, which is important information for data processors.

### **Application of Criterion 5 to Scott County Data**

A dipole sonic log was available reasonably close to the Scott County seismic survey. The  $V_p$  and  $V_s$  velocities read from this log are shown in Figure 6a. These velocity data were combined with a formation density log (Figure 6b) to construct a 2-D earth model that was, in turn, used to calculate the full-elastic data generated by a vertical-displacement source and recorded by vertical geophones. This earth model extended to approximately 4500 ft, the deepest depth coordinate of the dipole sonic log. The shallowest log measurement of P and S velocities and formation density was approximately 250 ft (Figure 6). Velocity and density

values between the earth surface and the depth of the onset of log measurements were assumed to be straight-line slopes that matched the depth-dependent trends in log-measured velocity and density across shallow strata. The straight-line trends of near-surface  $V_p$  and  $V_s$  velocities are shown in Figure 6a. The final earth model involved 300 velocity layers that were 15 ft thick. The source was buried at a depth of 30,000 ft to ensure no surface multiples appeared in the results. Receivers were extended to offsets of  $\pm 30,000$  ft with receiver stations spaced at intervals of 10 ft. This excessive offset was used so reflections from the edges of the model would not interfere with deep primary P-P and SV-P reflections that need to be examined.

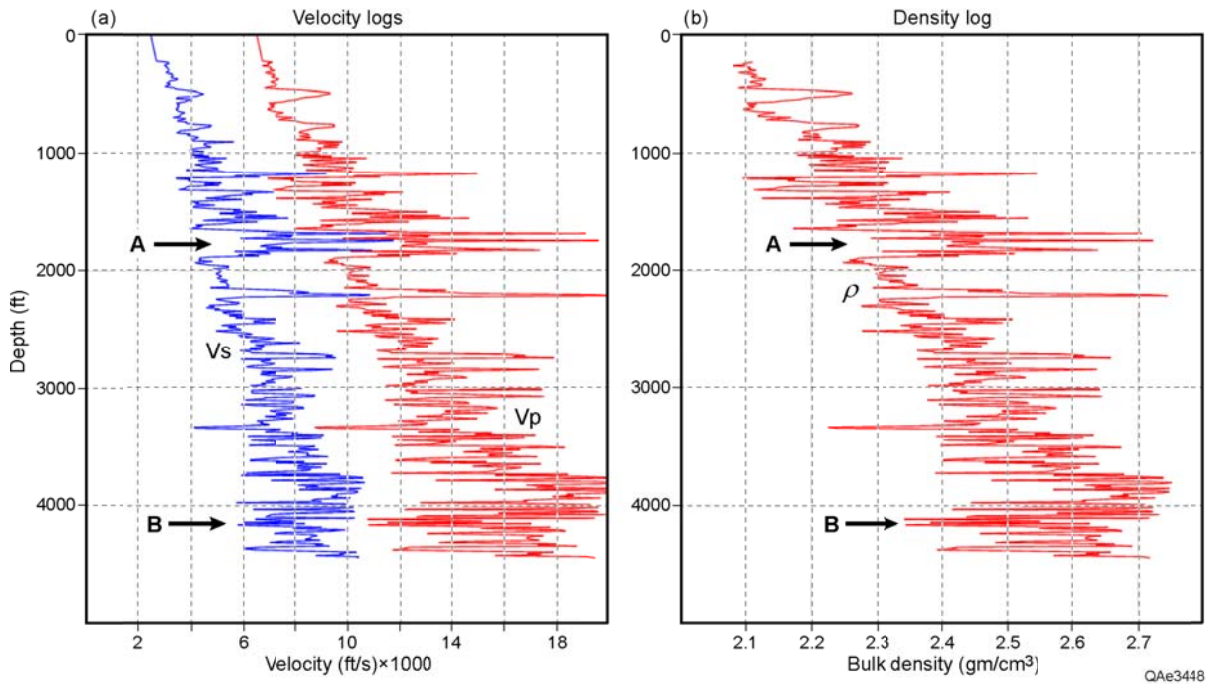


Figure 6. (a)  $V_p$  and  $V_s$  velocities and (b) bulk density log that defined the earth-model layering representing the seismic propagation medium for the the Scott County data. Intervals **A** and **B** produce strong reflection events.

Synthetic shot gathers were calculated from these log data, and velocity analyses were then performed on these gathers using the common procedure of creating constant-velocity stacks (Figure 7). A vertical-displacement source (vertical vibrator) was used to generate P-P constant-velocity stacks (Figure 7a), and a horizontal-displacement source (horizontal vibrator) was used to make SV-SV constant-velocity stacks (Figure 7b). The stacking velocity functions determined for these two types of shot gathers allowed a converted-mode stacking velocity to be calculated for the SV-P mode using the following relationship promoted by Tessmer and Behle (1988) and Iverson, et al., (1989):

$$(3) \quad (V_{SP})^2 = (V_{PP}) (V_{SS}) = (V_{PP})^2 (1/A)^{1/2},$$

In this equation,  $V_{SP}$  is SV-P stacking velocity,  $V_{PP}$  is the P-P stacking velocity shown in Figure 7a,  $V_{SS}$  is the stacking velocity shown in Figure 7b, and  $A$  is the velocity ratio  $V_{PP}/V_{SS}$ . The second form of the equation is appropriate for evaluating legacy P-wave data for SV-P data processing when one can obtain information only about  $V_{PP}$  and then is required to either know or guess an appropriate value ( $A$ ) for  $V_{PP}/V_{SS}$ .

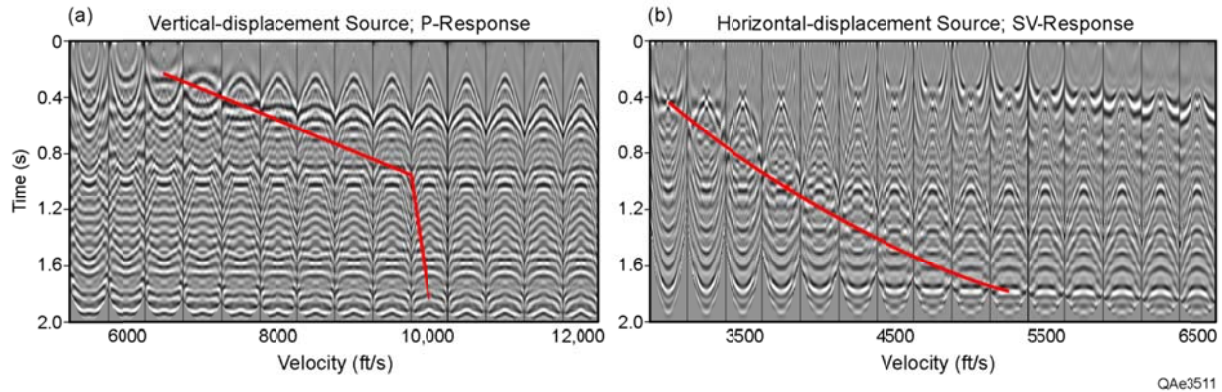


Figure 7. (a) P-P constant-velocity stacks created using a synthetic shot gather generated by a vertical-displacement source and recorded by vertical geophones. The red curve defines  $V_{PP}$  stacking velocity for a layered earth described by the log data in Figure 6. (b) SV-SV constant-velocity stacks created using a synthetic shot gather generated by a horizontal-displacement source and recorded by horizontal geophones. The red curve defines  $V_{SS}$  stacking velocity for a layered earth represented by the log data in Figure 6.

The log data in Figure 6 show there are two intervals of dominating impedance contrasts in the earth layering across the Scott County legacy survey: (1) a shallow interval, labeled **A**, that creates a P-P reflection  $A_{PP}$  and a SV-P reflection  $A_{SP}$ , and (2) a deep interval, labeled **B**, that creates a P-P reflection  $B_{PP}$  and a SV-P reflection  $B_{SP}$ . The principal target of interest at this Scott County site is the deep interval identified as **B**.

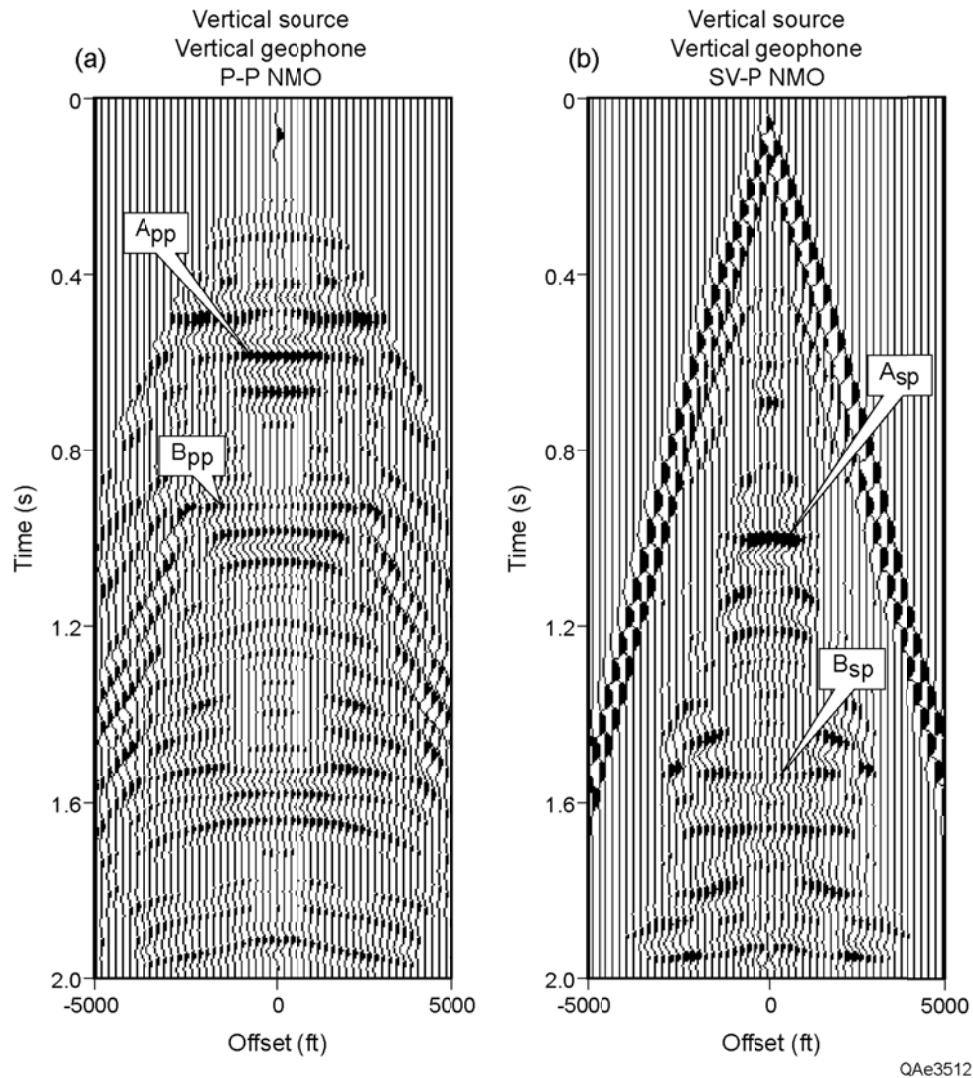


Figure 8. Shot gathers generated by a vertical-displacement source and recorded by vertical geophones. (a) Shot gather after a P-P NMO is applied to flatten P-P reflections. Key reflections  $A_{pp}$  and  $B_{pp}$  are identified. (b) Shot gather after a SV-P NMO is applied to flatten SV-P reflections. Reflections  $A_{sp}$  and  $B_{sp}$  are depth equivalent to P-P reflections  $A_{pp}$  and  $B_{pp}$ , respectively.

The shot gathers in Figure 8 were generated from the log data in Figure 6 using a vertical-displacement source to represent the vertical vibrator source that acquired the Scott County data. Figure 8a shows the response of the vertical geophones after a P-P NMO has been applied to flatten P-P reflections. This P-P NMO function is based on the P-P stacking velocity interpreted from the P-P constant-velocity stacks in Figure 7a. Key reflection events  $A_{pp}$  and  $B_{pp}$  are labeled. The shot gather in Figure 8b shows the response of the vertical geophones when a SV-P NMO is applied. This SV-P NMO correction is determined from the  $V_{sp}$  stacking velocity defined in Equation 3. Reflection events  $A_{sp}$  and  $B_{sp}$  are depth-equivalent to P-P events  $A_{pp}$  and  $B_{pp}$  in Figure 8a.

The key result of this modeling is that SV-P reflections  $A_{SP}$  and  $B_{SP}$  are reasonably isolated from interference with P-P reflections and multiples. Thus it should be possible to extract a good-quality SV-P image and valid S-wave attributes from the Scott County data IF SV-P reflections existed in the data. However, Criterion 3 discussed earlier demonstrated SV-P reflections are not present because inappropriate sweep parameters were used to operate the vibrator sources (Figure 5).

### **Criterion 6 - Physical Sizes of Source and Receiver Arrays**

The ideal physical sizes of source and receiver arrays used to acquire S-mode data are a single-point source station and a single-point receiver station. Examples of a single-point source station would be a single shot-hole or a single vertical vibrator operated with no move-up while generating an illuminating wavefield. A single-point receiver would be only one geophone at each receiver station. The logic involved in using minimal-dimension source and receiver stations for acquiring S-mode data is that at some sites, S-wave statics can vary in such short distances that one has to be concerned about intra-array variations in S statics if either source-station arrays or receiver-station arrays span an appreciable distance.

Intra-array statics refer to static changes that occur in distances that are shorter than the physical dimensions of a receiver array or a source array. It is now a widely accepted principle that S statics often vary over shorter distances than do P statics, thus the physical sizes of P-P source and receiver arrays have to be considered in SV-P data processing even though those array sizes may not be a concern in P-P data processing. Because the physical dimensions of source arrays and receiver arrays have not been a serious concern in acquiring most P-P data surveys, large-dimension source arrays and receiver arrays will often be encountered when reviewing legacy P-P data for possible SV-P data processing. When considering P-P data options, EGL's philosophy is, assuming that all other factors are equal, choose the data that were acquired with the smallest source-station and receiver-station dimensions.

### **Application of Criterion 6 to Scott County Data**

The sources that generated the Scott County data were two inline vertical vibrators with baseplates separated a distance of 40 ft. Although a single vibrator would be a more optimal source for SV-P imaging, this vibrator pair is a reasonable approximation of a point source.

The receivers that recorded the Scott County data were six vertical geophones deployed in a circle having a diameter of 12 ft. These six geophones are a reasonable approximation of a point receiver.

### **Criterion 7 – Signal-to-Noise Character of SV-P Reflections**

An example showing how SV-P reflections can be located in constant-velocity stacks of vertical-geophone data has been illustrated in Figure 5, but the logic used to identify the search-window position where SV-P reflections should appear in these velocity panels was

not discussed in detail in the text accompanying that figure. The important fact that the signal-to-noise ratio of SV-P reflections can be evaluated with common CMP-based P-wave velocity panels now needs to be discussed and will be illustrated using better quality data than the data that were used in Figure 5. In order to judge the signal-to-noise character of SV-P reflections, it is essential to know how to locate those SV-P reflections in CMP-based constant-velocity stacks of vertical-geophone data.

### **Application of Criterion 7 to Scott County Data**

The application of Criterion 7 to the Scott County data has been illustrated in Figure 5. The constant-velocity CMP vertical-geophone stacks shown in that figure confirm that the signal-to-noise ratio of the strongest SV-P reflection (feature labeled  $A_{SP}$ ) expected to exist at each velocity analysis location is quite low. A valid question to ask at this point is “*why should SV-P reflections, which need to be created using asymptotic conversion point (ACP) binning, even be seen in CMP-based constant-velocity stacks*”? This question will be answered in this section.

The CMP velocity panels in Figure 5 were included in the discussion of Criterion 3 to confirm that the decision to not go forward with SV-P processing, based only on the undesirable vibrator sweep parameters that were used, was a correct decision. However, an important principle now needs to be emphasized about CMP constant-velocity stacks. This **principle** is that *regardless of how compelling the logic is that any of the criteria discussed in this report indicate SV-P data processing should not be initiated, it is still advisable to acquire, or to create, CMP constant-velocity stacks of vertical-geophone data that will allow the signal-to-noise character of SV-P reflections to be examined.*

The data examples in this section illustrate EGL’s current procedure for defining the positions of SV-P reflections in CMP-based constant-velocity-stack panels. The concepts used to analyze CMP constant-velocity stacks are illustrated in Figure 9. First, the  $V_P/V_S$  ratio needs to be known or assumed (Figure 9a). For legacy P-P data, constant-velocity panels are created using common-midpoint (CMP) procedures (Figure 9b). Equation 3 is then used to define the SV-P CMP stacking velocity  $V_{SP}$  that corresponds to P-P stacking velocity  $V_{PP}$ . The term  $A$  in Equation 3 is the  $V_P/V_S$  value associated with P-P stacking velocity  $V_{PP}$  illustrated in Figure 9a. A second key equation that relates the image-time coordinate of P-P reflection PP1 in constant-velocity panel  $V_{PP1}$  to the image-time coordinate of SV-P reflection SP1 in constant-velocity panel  $V_{SP1}$  is

$$(4) \quad T_{SP} = 0.5 T_{PP} (A + 1)$$

This equation is developed in Figures 9c and 9d.

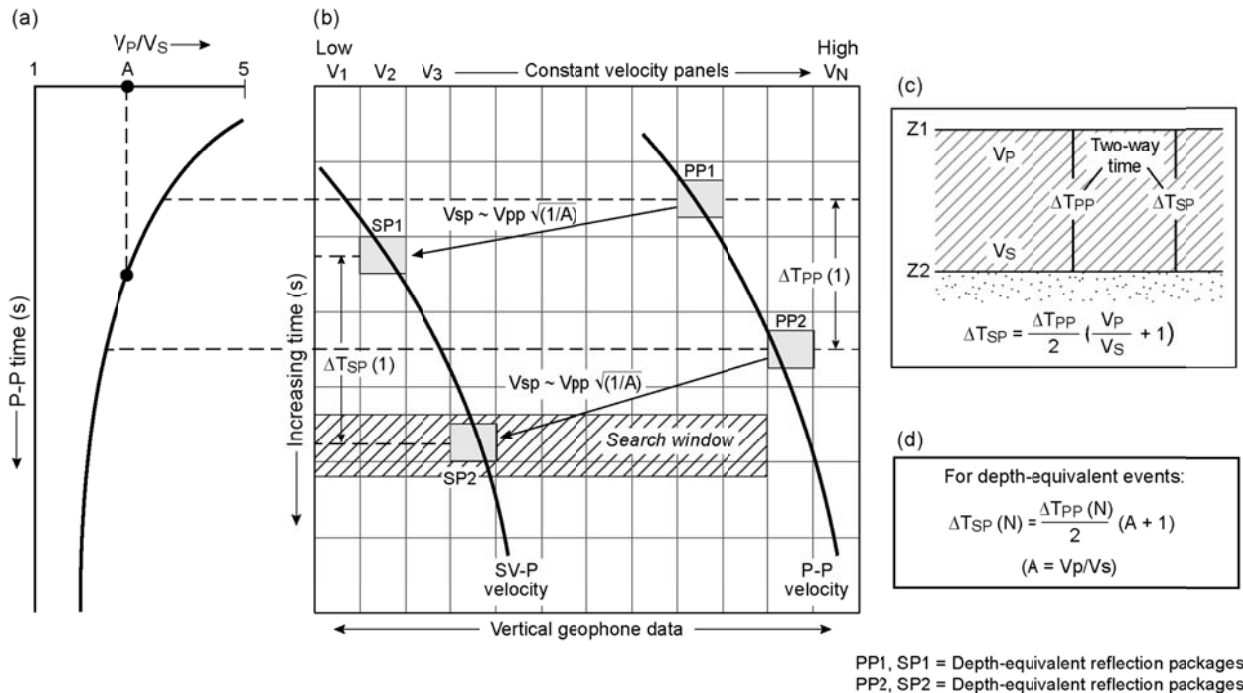


Figure 9. (a) An averaged  $V_p/V_s$  velocity ratio function known (or assumed) for a prospect of interest. (b) A hypothetical panel of P-P constant-velocity stacks created by CMP binning (not ACP binning!) at a CDP location in the seismic image space of that prospect. The P-P stacking velocity determined at this CDP by a data processor is shown on the right side of this panel. (c) Model showing relationship between 2-way P-P and SV-P times across a target interval. (d) Mathematical equation expressing the travel time relationships between depth-equivalent P-P and SV-P reflections at depths  $Z_1$  and  $Z_2$ . This equation is used to define search windows in the constant-velocity stack panel where SV-P reflections that are depth-equivalent to targeted P-P reflections should be positioned.

Because SV-P data should be binned using asymptotic-conversion-point (ACP) procedures, a key question is whether these two simple equations (Equations 3 and 4) can be used to confirm that SV-P reflections exist in CMP-based (not ACP-based) constant-velocity stacks. The answer is “yes”. This is a fortunate outcome that is invaluable when faced with the challenge of verifying that SV-P reflections exist in legacy P-P data.

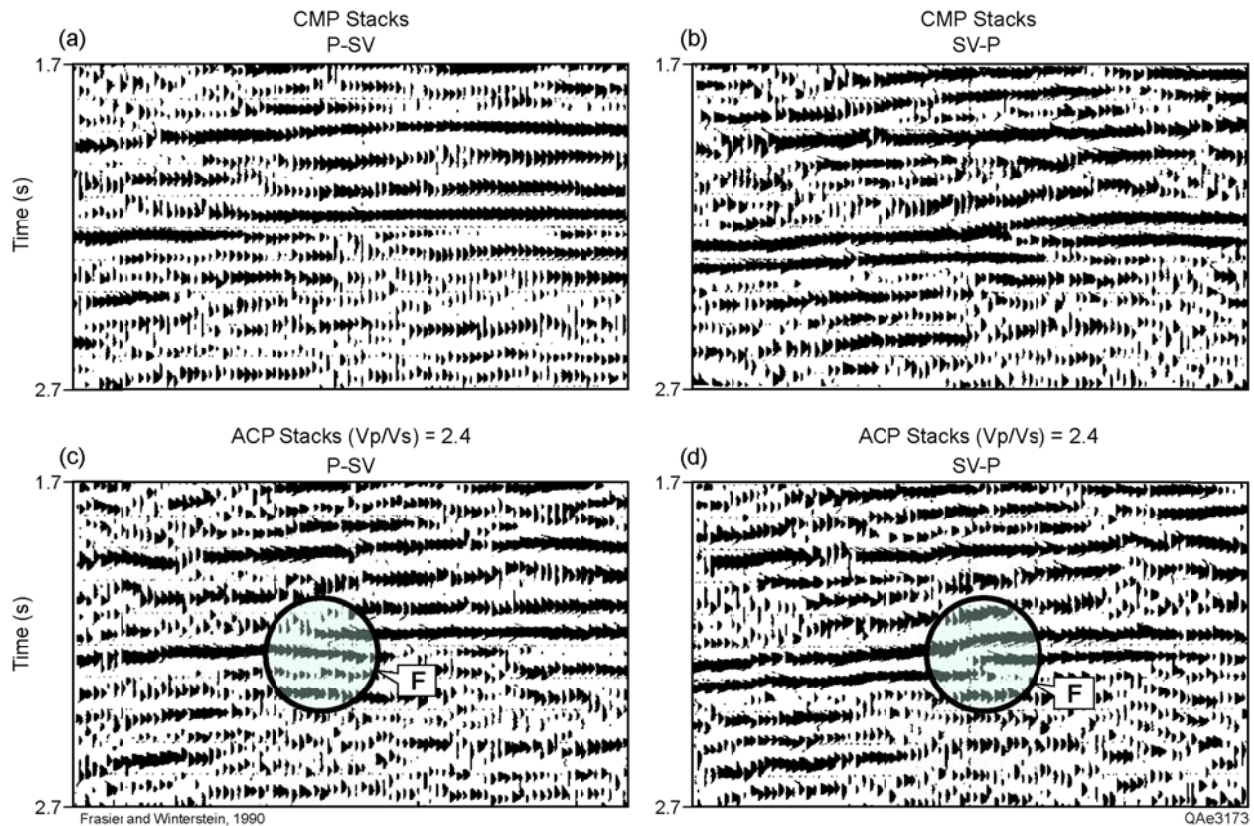
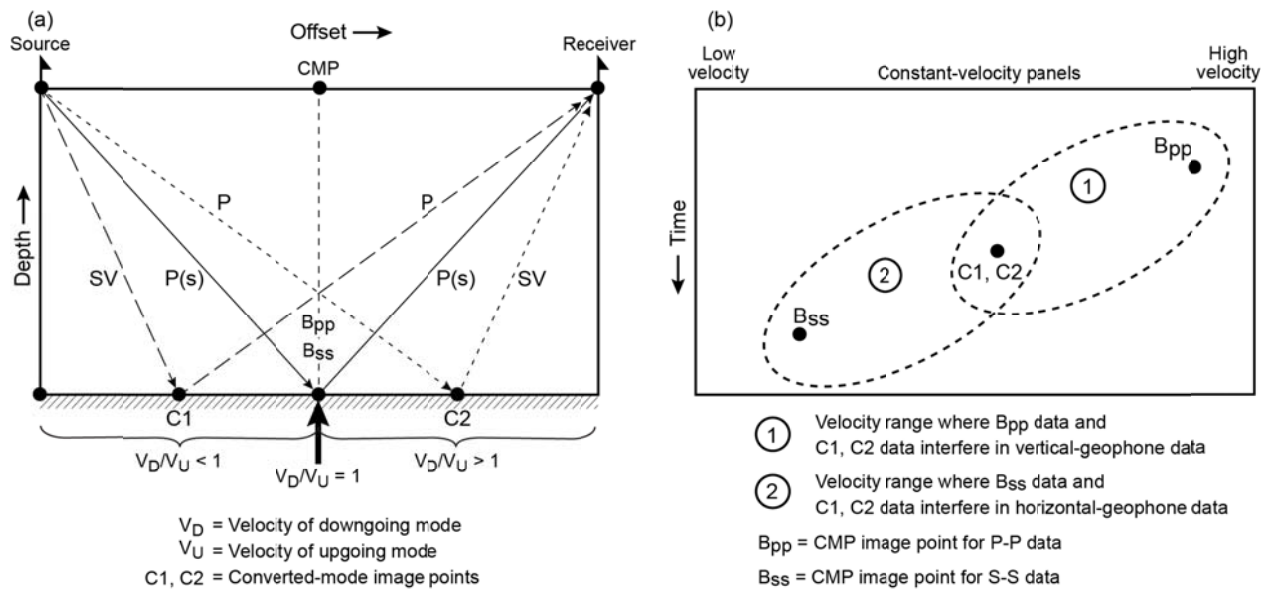


Figure 10. (a) P-SV image constructed with CMP binning techniques. This CMP imaging effort is equivalent to ACP binning of horizontal-geophone data using a  $V_p/V_s$  velocity ratio of 1. (b) SV-P image made using CMP binning techniques. This CMP image is equivalent to assuming  $V_p/V_s = 1$  when performing ACP binning of vertical-geophone data. (c) P-SV image made with ACP binning and a  $V_p/V_s$  value of 2.4. (d) SV-P image made with ACP binning and a  $V_p/V_s$  value of 2.4. Taken from Fraiser and Winterstein, 1990. Window F emphasizes a fault the authors used to verify the accuracy of each image.

An important principle observed by EGL is that SV-P reflections do indeed appear in P-P CMP-based constant-velocity stacks of vertical-geophone data. Although these reflections are not optimal for SV-P imaging purposes (because they are not based on ACP binning), they are visible with sufficient signal-to-noise character to confirm if SV-P reflections exist and whether SV-P data processing should, or should not, be initiated. This key fact, that converted-mode images can be made using CMP procedures rather than ACP procedures, has been documented by Fraiser and Winterstein (1990). Figure 21 from their paper is repeated here as Figure 10. It must be emphasized that converted-mode images made with CMP binning, as are those in Figures 10a and 10b, are inaccurate images because reflection points are not properly positioned in image space. In contrast, the converted-mode images in Figures 10c and 10d are made with ACP binning and a proper  $V_p/V_s$  value of 2.4 for the area where these data were acquired. These latter images show the correct position of fault F. A principle illustrated by these data is “if an SV-P reflection made with CMP stacking procedures has reasonable signal-to-noise, when that same SV-P reflection is created with ACP stacking procedures and a correct value of  $V_p/V_s$ , it will have even better signal-to-noise character”. Thus the presence of any

reasonable-quality reflection positioned at the correct velocity-time coordinates in CMP constant-velocity stacks of vertical-geophone P-P data is sufficient evidence to warrant initiating SV-P data processing of those P-P data.

One way to understand why SV-P reflections occur in P-P CMP velocity panels of vertical-geophone data is to view constant-velocity stacks of the data as an SV-P stacking process in which a data processor has simply made an inaccurate assumption as to the value of the  $V_P/V_S$  ratio that should be used to image SV-P data. In fact, the processor has applied the worst possible value of  $V_P/V_S$ , that being a value of 1. Thus if an SV-P reflection is recognized when  $V_P/V_S = 1$ , that reflection will exhibit better and better signal-to-noise as the  $V_P/V_S$  ratio is adjusted toward the proper velocity-ratio value for the prospect area where legacy P-P data have been acquired.



QAe3445

Figure 11. (a) The position of an image point along an interface depends on the velocity ratio  $V_D/V_U$ , where  $V_D$  is downgoing velocity and  $V_U$  is upgoing velocity. CMP imaging occurs when  $V_D/V_U = 1$ . (b) CMP reflections and converted-mode reflections overlap in two general areas on a constant-velocity panel, the areas labeled 1 and 2.

The diagram in Figure 11a illustrates this concept in terms of the velocity ratio  $V_D/V_U$ , where  $V_D$  is the velocity of a downgoing illuminating wavefield, and  $V_U$  is the velocity of an upgoing reflected wavefield created by that illuminating wavefield. CMP imaging is just one of the many coordinate positions along the horizontal  $V_D/V_U$  axis where an image point can be located in the full range of velocity-ratio possibilities. Specifically, CMP stacking occurs only when  $V_D/V_U = 1$ ; whereas, SV-P stacking involves conditions where  $V_D/V_U < 1$ , and P-SV stacking involves conditions where  $V_D/V_U > 1$  (Figure 11a).

Figure 11b defines the areas in constant-velocity-stack data space where there will be both CMP reflections and converted-mode reflections. Note that only area **1** in Figure 11b involves SV-P data and legacy P-P data. Area **2** involves constant-velocity stacks made with horizontal-geophone data where P-SV and SV-SV reflections interact with each other.

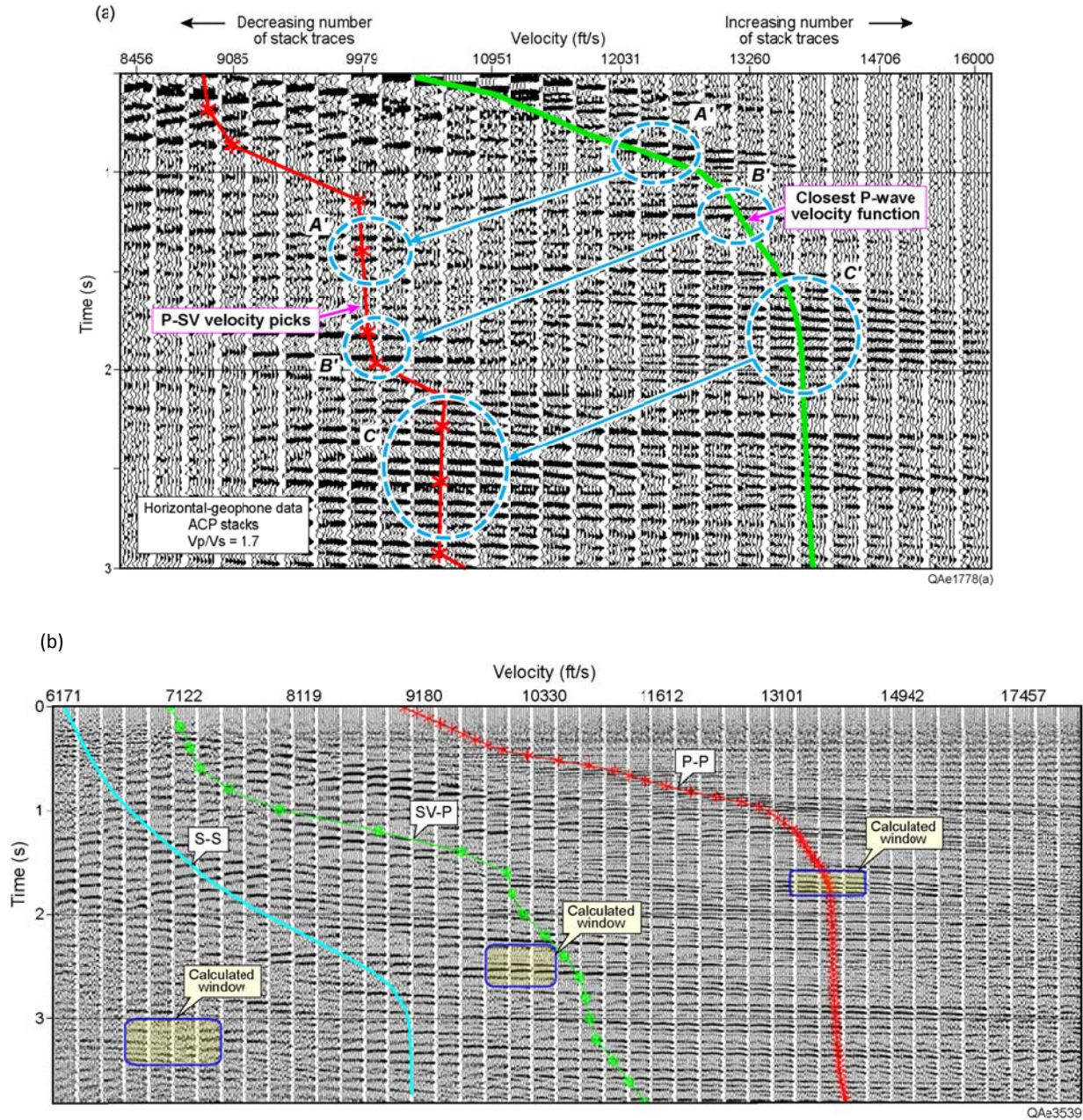


Figure 12. (a) Constant-velocity ACP stacks constructed from horizontal-geophone data. Depth-equivalent P-P and P-SV reflections are shown by connecting arrows. (b) Constant-velocity CMP stacks made from vertical-geophone data. Reflections in these vertical-geophone data extend from the P-P stacking function to the SV-P stacking function, and possibly even to the SV-SV stacking function.

Real data examples of constant-velocity stacks that confirm the concepts presented in Figure 9 through 11 are shown in Figure 12. The data in Figure 12a are constant-velocity ACP (asymptotic conversion point) stacks of horizontal-geophone data. Although the topic of this report is extracting SV-P reflections from vertical-geophone data, this horizontal-geophone data example is so impressive that it needs to be shown. Two stacking velocity curves are shown. The left-side curve is the ACP P-SV stacking velocity determined at the CDP where these data were analyzed, and the right-side curve is the P-P stacking velocity that was determined from CMP stacks of vertical-geophone data at this same CDP location and then inserted onto this horizontal-data velocity panel. Visual inspection of these data allows one to conclude that the circled P-P and P-SV reflection packages represent images of the same geology; i.e., the P-P and P-SV reflection pairs linked by connecting arrows are depth-equivalent reflections. This example shows that both P-P and converted-mode reflections can be seen not only in constant-velocity CMP stacks, but also in ACP constant-velocity stacks. This fact is particularly impressive because it is often assumed that P-P reflections cannot be seen in horizontal-geophone data, but obviously in some instances, this assumption is not correct.

Returning now to the topic of this report, the data in Figure 12b are constant-velocity CMP stacks constructed from vertical-geophone P-P data. The P-P velocity function is on the right, the SV-P stacking velocities determined at this CDP are shown by the curve in the center, and a tentative SV-SV stacking velocity function determined from horizontal-geophone data is shown on the left. The positions of the depth-equivalent SV-P and SV-SV data windows drawn on the velocity panel were calculated using Equations 3 and 4 and a  $V_P/V_S$  value of 1.9. These calculated positions of expected SV-P and SV-SV reflections imply that these particular SV-P and SV-SV stacking-velocity curves “may” be slightly too fast. Even so, this real-data example verifies the principle that SV-P reflections, and sometimes (but not always) SV-SV reflections, exist in CMP constant-velocity stacks made from vertical-geophone data.

In summary, once good-quality P-P reflections are identified at image times PP1 and PP2 in a panel of CMP-based constant-velocity stacks of vertical-geophone data (Figure 9), the 2-step procedure for identifying the search windows where depth-equivalent SV-P reflections SP1 and SP2 should be found is:

1. Move horizontally along the stacking velocity axis from velocity panel PP1 (or PP2) to a slower velocity panel defined by Equation 3, and then,
2. Move vertically down the image-time axis to a later image time defined by Equation 4.

Although this procedure defines the expected location of the depth-equivalent SV-P reflection in a suite of CMP constant-velocity panels, a modest sized search window should be centered on this calculated SV-P reflection location as illustrated in Figures 9 and 12b to allow for some estimation error.

## **Criterion 8 – SV-P Reflections Embedded in VSP Data**

If vertical seismic profiling (VSP) data are available at a legacy P-P data site of interest, analysis of those data can provide valuable evidence of the presence of SV-P reflections and the quality of those reflections. However, the effort to process VSP data approaches the effort required to process surface-based data so a decision to process VSP data before processing surface data is not to be taken lightly.

A second point is that no one other than EGL has ever extracted SV-P reflections from VSP data. Thus VSP data-processing assistance is only beginning to emerge across the industry because of the technical advance in VSP data processing that is just now being publicized by EGL. Rather than consume space here to explain the nuances of VSP SV-P data processing, readers are referred to the paper by Li and Hardage (2015) that discusses how SV-P reflections are extracted from VSP data. This paper is available by request or can be found by going to the EGL Web site – <http://www.beg.utexas.edu/egl/> - and clicking on **Publications**.

## **Application of Criterion 8 to Scott County Data**

No VSP data were available local to the Scott County study site. Criterion 8 could not be applied to the Scott County P-P legacy data.

## **Conclusions**

This report summarizes the criteria that need to be considered when deciding whether a particular P-P legacy data set should be reprocessed to create SV-P data. These criteria were applied to a real P-P legacy seismic survey acquired in Scott County, Kansas, to decide if those data were candidates for SV-P data processing. These particular P-P data had serious shortcomings. First, the trace length was not sufficient. Second, there was inadequate low-frequency energy in the SV illuminating wavefield created by the vertical vibrator source. This inadequate low-frequency energy was caused by a vibrator sweep that started at 12 Hz, rather than at 4 Hz or 6 Hz, and that then proceeded through the low-frequency range of vibrator-pad motion at a rapid rate of 3dB per octave. The direct-S mode created by this sweep had inadequate low-frequency energy to produce robust SV-P reflections that would image geologic targets.

Considerable attention is focused in this report on analyzing constant-velocity CMP stacks of vertical-geophone data to recognize SV-P reflections in legacy P-P data. This data criterion – examining constant-velocity CMP stacks – is one of the most definitive of all the criteria that can be used to decide if SV-P data processing should be initiated. After applying all of these data-evaluation criteria to the Scott County data, we found no evidence that SV-P reflections had sufficient signal-to-noise to justify SV-P data processing.

All criteria discussed in this report are condensed into a concise tabulation appended as Table 1 at the end of this document.

### References

Frazier, C., and D. Winterstein, 1990, Analysis of conventional and converted mode reflections at Putah sink, California using three-component data: *Geophysics*, 55, 646-659.

Iverson, W.P., B.A. Fahmy, and S.B. Smithson, 1989,  $V_pV_s$  from mode converted P-SV reflections: *Geophysics*, 54, 843-852.

Li, Y, and B. Hardage, 2015, Extraction and imaging of SV-P reflections from far-offset VSP data: undergoing peer review for publication in the SEG-AAPG journal **Interpretation**. Available at the EGL Web site, <http://www.beg.utexas.edu/egl/>.

Tessmer, G., and A. Behle, 1988, Common reflection point data stacking technique for converted waves: *Geophys. Prosp.*, 36, 671-688.

Table 1: Criteria for Evaluating Legacy P-P Data

CRITERION	ACTION STEP	DECISION
Trace length	Define P-P image time $T_{pp}$ of deepest target	Do data extend to position of SV-P reflection at far offset? $T_{sp} = 0.7 (1 + V_p/V_s) T_{pp}$
SV-P acquisition footprint	Calculate P-P and SV-P fcid at various depths	<ul style="list-style-type: none"> <li>• Are undesirable footprint effects present?</li> <li>• Do superbins have to be utilized?</li> </ul>
Low-frequency energy	<ul style="list-style-type: none"> <li>• Calculate frequency spectrum</li> <li>• Determine linear or non-linear sweep</li> <li>• Determine start frequency <math>\leq 6</math> Hz</li> <li>• Construct constant-velocity stacks and evaluate quality of SV-P reflections</li> </ul>	<ul style="list-style-type: none"> <li>• Are sufficient low-frequency data present?</li> <li>• Are SV-P reflections evident?</li> </ul>
S-wave statics	<ul style="list-style-type: none"> <li>• Analyze all static issues</li> <li>• Attempt trial inversions of Rayleigh wave for <math>V_p</math> and <math>V_s</math></li> </ul>	<ul style="list-style-type: none"> <li>• Rayleigh wave suitable for inversion?</li> <li>• Obvious shallow refractors?</li> </ul>
Size of source and reservoir arrays	<ul style="list-style-type: none"> <li>• Review acquisition parameters</li> </ul>	<ul style="list-style-type: none"> <li>• Small arrays are desired to avoid intra-array statics</li> </ul>
Interfering reflections	<ul style="list-style-type: none"> <li>• Calculate synthetic data (1D and 2D)</li> <li>• Apply NMO to synthetic responses of vertical geophones</li> </ul>	<ul style="list-style-type: none"> <li>• Do SV-P reflections from shallow interfaces interfere with P-P reflections from deep interfaces?</li> <li>• Can P-P and SV-P wavefields be separated?</li> </ul>
Signal-to-noise character of SV-P reflections	<ul style="list-style-type: none"> <li>• Obtain or create constant-velocity stacks of vertical-geophone data</li> <li>• Locate reflections on slow-velocity panels</li> </ul>	<ul style="list-style-type: none"> <li>• Are SV-P reflections present?</li> <li>• Are SV-P reflections robust?</li> </ul>
VSP evidence	Obtain and process local VSP data	<ul style="list-style-type: none"> <li>• Are SV-P reflections present?</li> <li>• Are SV-P reflections robust?</li> <li>• How severe is the interference between P-P and SV-P reflections?</li> </ul>

QAe3446